NOTES AND CORRESPONDENCE

Numerical Simulation of Wind Hole Circulation at Ice Valley in Korea Using a Simple 2D Model

H. L. TANAKA

Center for Computational Sciences, University of Tsukuba, Tsukuba, Japan

Daisuke NOHARA

APEC Climate Center, Busan, South Korea

and

Hi-Ryong BYUN

Department of Environmental Atmospheric Sciences, Pukyong National University, Busan, South Korea

(Manuscript received 31 March 2006, in final form 24 August 2006)

Abstract

In this study, numerical simulations of the summertime ice formation at Ice Valley in Korea are conducted using a simple 2D model, which is driven by the observed air temperature. The Ice Valley in Korea is a famous summer resort, as the Natural Monument where natural ice forms in spring, and remains till summer along the slope, and the ice disappears in fall to winter. It is interesting to note that the hotter the outside air is, the larger the ice grows in spring. The mysterious behavior of the summertime ice has been partly explained by a series of numerical experiments in terms of the convection theory, which is explained by the seasonally reversing wind-hole circulations. The numerical model in this study is updated from our former versions considering the new finding by the in situ observations. The result of the simulation is compared with the observations at the Ice Valley in Korea, and Nakayama in Japan.

According to the result of the numerical simulation, the summertime wind-hole circulation activates the downward flow when the outside air is getting hot. The downward flow transfers the cold accumulated in the talus during the previous winter toward the outlet of the cold wind hole. As a result, the intensified cold advection grows the ice when the outside air is getting hot. The wind hole circulation appears to be about 17 mm/s in April, and the residence time of the air in the talus is estimated as 2.8 hours for this case. It is shown, that the seasonal reversal of the wind hole circulation is the essential mechanism of the summertime ice at the Ice Valley, acting as a natural thermal filter which effectively accumulates only the winter cold in the talus.

Corresponding author: Hiroshi L. Tanaka, Center for Computational Sciences, University of Tsukuba, 1-1-1 Tennodai, Tsukuba, Ibaraki 305-8572, Japan.
E-mail: tanaka@sakura.cc.tsukuba.ac.jp

1. Introduction

The Ice Valley (Eorumgol) in Korea is a famous summer resort, where natural ice forms in spring and summer, and the ice disappears in fall and winter (see Hwang and Moon 1981;

Bae and Kayane 1986; Song 1994; Tanaka 1995; Hwang et al. 2005; Byun et al. 2006). It is interesting to note that the hotter the outside air is, the larger the ice grows in spring and maintains till summer, as reported by Kim (1968). The ice partially melts after a rainfall, due to the warmth of the rain, but it freezes again after a few days in spring. In contrast, there is no ice in the talus during winter, despite the fact that the surrounding mountains are covered by snow (see Byun et al. 2006).

Ice Valley (128°59′E, 35°34′N) is the Natural Monument located in the upper reaches of the Milyang River (a branch of the Nakdong River) in the northern part of Milyang, Kyungnam, which is in the south-eastern part of the Korean Peninsula (see Fig. 1). The valley is about 250 m wide and 750 m long, with a slope of 15–25 degrees. The slope of the talus is covered by dacite welded ash flow tuff, which are about 0.5–2.0 m in diameter. The freezing area in the Ice Valley is located near 410 m above sea level at the very lower end of a widely spreading ash fall tuff debris, as marked by a circle in Fig. 1 (after Tanaka 1997). Extensive observational studies were conducted and reported by Tanaka et al. (1998, 1999), Hwang et al. (2005), and Byun et al. (2006).

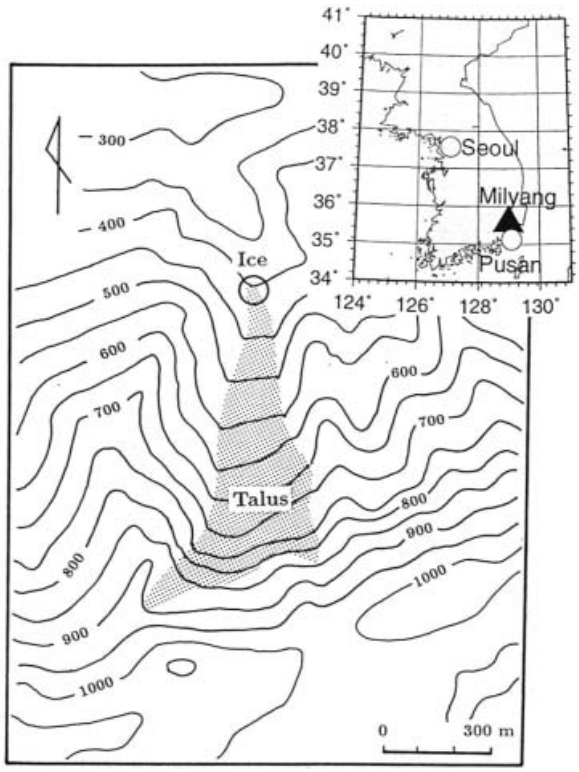

Fig. 1. Location of the Ice Valley in Milyang, Korea. The talus area is shaded. The Ice Valley's ice is located at the bottom of the talus near the 410 m level marked by a circle (after Tanaka 1997).

The mysterious behavior of the summertime ice has been explained by (1) adiabatic expansion of air blowing from the narrow holes (Kim 1968), (2) evaporation from capillary zone above the ground water (Moon and Hwang 1977), (3) convection of cold air during winter (Bae and Kayane 1986), (4) net radiative cooling and cold air convection in winter (Hwang et al. 2005). The summertime ice formation is partly explained by a series of numerical experiments by Tanaka et al. (2000), in terms of the convection theory with a seasonal reversal of wind-hole circulations. While the downward flow of cold air takes place gently in summer, a violent overturning of the air occurs in winter, by the unstable stratification. According to the model simulation, the seasonal asymmetry of the wind-hole circulations acts as a natural thermal filter, which effectively accumulates only the cold in winter into the talus. The circulation speed inferred by the model was 1 mm/s, with the residence time of 2 days in the talus.

In order to quantitatively confirm the wind-hole circulations in the talus, tracer experiments were conducted by Tanaka et al. (2004), using dry ice as the safe and harmless tracer. According to the results of the tracer experiments, the wind-hole circulation in summer turns out to be 26 mm/s, with the residence time of only 90 minutes, which contradicts with the model speculation. Apparently, the model simulation must be updated with the observational facts.

Extensive and comprehensive in situ observations of the Ice Valley were carried out by Byun et al. (2004) for April 2003 to May 2004, showing the typical characteristics of warm wind holes at the upper slope of the talus. The warm wind hole was identified by Tanaka et al. (2000) as the Nakayama Wind Hole in Japan, and was simulated successfully under the constrained air flow in the talus. However, the characteristics of the warm wind hole were absent in the model simulation for the Ice Val-

ley, due to the violent overturning of the air in winter. In this respect as well, the numerical model must be modified, so as to agree with the observations.

The purpose of this study is to update the numerical model simulation of the Ice Valley by Tanaka et al. (2000), based on the tracer experiments by Tanaka et al. (2004), and the in situ observations by Byun et al. (2004). We apply the Nakayama model to the Ice Valley, assuming a prescribed air route in the talus in order to represent the characteristics of the warm wind hole. The model is driven by the actual outside air temperature, and the parameters are adjusted so that the circulation speed coincides with the observation by the tracer experiments. It is our goal to understand the mechanism of the Ice Valley's ice, which forms in spring and summer and disappears in fall and winter, and which grows (shrinks) under the hotter (cooler) outside air in spring. Section 2 describes the 2D model equations, and the results of the numerical simulation are presented in Section 3. Concluding summary for the mechanism of the Ice Valley's ice is given in Section 4.

2. Description of the model

The numerical model used in this study is documented in detail by Tanaka et al. (2000), so a brief description is presented here. Figure 2 illustrates a schematic cross section of the talus, which is composed of large boulders with plenty of space where air can penetrate freely.

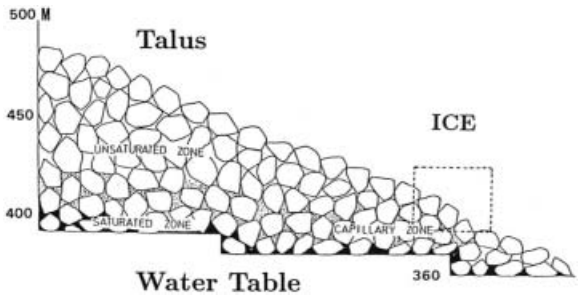

Fig. 2. Schematic cross section of the talus composed by large boulders. An unsaturated capillary zone is formed above the water table. The Ice Valley's ice is located in the squared-box area (after Moon and Hwang 1977).

The Ice Valley's ice is located at the lower slope of the talus, specified by the box. An unsaturated capillary zone is formed above the water table (after Moon and Hwang 1977).

The numerical model for the inclined porous media consists of: the equation of motion; hydrostatic equation; mass continuity; and, thermodynamic energy equation for air and the talus (rocks). It is a two dimensional model in horizontal (x-coordinate) and vertical (z-coordinate) directions, and the talus is located at the lower left corner of the model domain. The soil (or rock) temperature in the talus is governed by heat exchange, with the air flowing into the talus as follows:

$$\nu u = -RT_a \frac{\partial \ln p}{\partial x}, \tag{1}$$

$$\frac{\partial \ln p}{\partial z} = -\frac{g}{RT_a}, \tag{2}$$

$$\frac{\partial u}{\partial x} + \frac{\partial w}{\partial z} = 0, \tag{3}$$

$$\frac{dT_a}{dt} = -\frac{g}{c_p} w - \frac{\alpha}{c_p}(T_a - T_s) + K_a \nabla^2 T_a, \tag{4}$$

$$\frac{\partial T_s}{\partial t} = -\frac{\alpha M}{c_s}(T_s - T_a), \tag{5}$$

where

$$\frac{d}{dt} = \frac{\partial}{\partial t} + u\frac{\partial}{\partial x} + w\frac{\partial}{\partial z}. \tag{6}$$

The variables are air temperature T_a, soil (rock) temperature T_s, horizontal and vertical wind speeds u, w, and atmospheric pressure p. The parameters are specific heat for rocks c_s specific heat c_p and gas constant R for dry air, gravity acceleration g, Rayleigh friction coefficient ν, Newtonian cooling coefficient α, effective mixing ratio of air to rocks M, and diffusion coefficients of the air K_a, respectively.

The momentum equation (1) represents a balance between pressure gradient force and Rayleigh friction. The hydrostatic assumption (2), and incompressibility (3) may be acceptable for very slow laminar flow of the order 10 mm/s. In (4) the right hand side represents adiabatic compression by the vertical motion, Newtonian cooling relaxing to T_s, and thermal diffusion. As represented by the right hand side of (5), the same amount of heat energy is

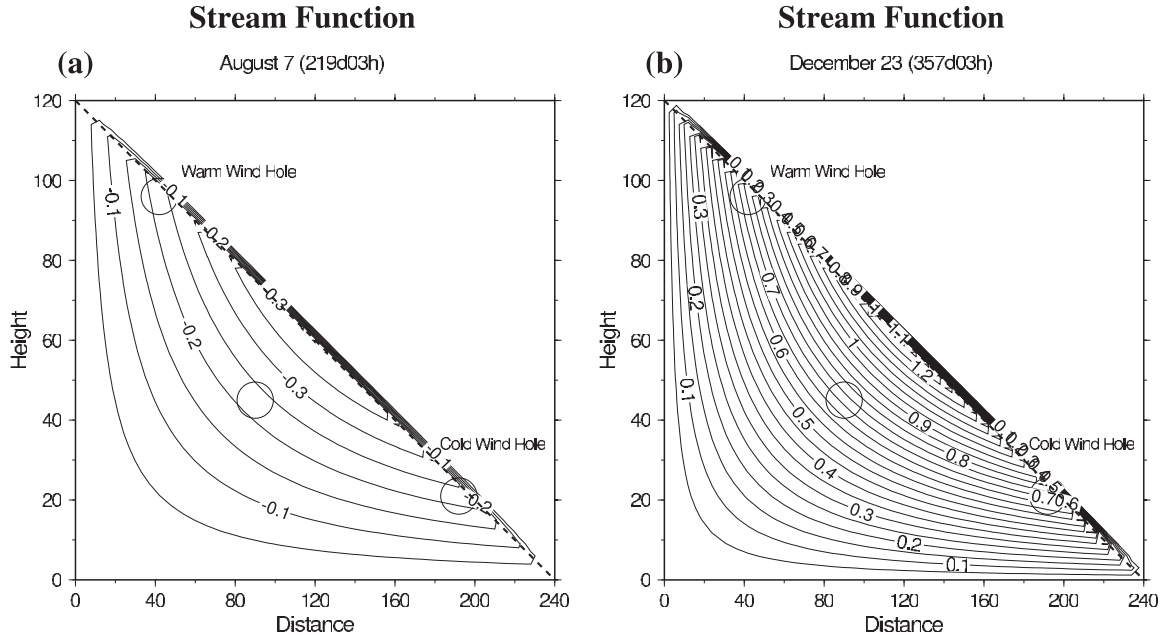

Fig. 3. Vertical cross sections of stream function (m^2s^{-1}) in the model for (a) August 7 (day 219) and (b) December 23 (day 357) at 0300 LST. The cold wind hole, warm wind hole, and interior talus are represented by the points at the distance $(192, 21)$, $(42, 96)$, and $(90, 45)$, respectively, as marked by circles.

used conversely to warm or cool the rocks, in order to conserve heat energy. A simple ice thermodynamics is introduced so that the temperature is fixed at the freezing point when freezing or melting occurs (see Tanaka et al. 2000). Note that the driving force for the wind-hole circulation is not the buoyancy of an air parcel along the vertical coordinate, but a horizontal pressure gradient induced by the temperature contrast.

We assume that the background pressure is constant at the top of the model domain. Given a temperature distribution, the hydrostatic equation (2) is integrated with respect to height, to obtain the horizontal pressure gradient in (1). Horizontal wind speed is then diagnostically evaluated from the pressure gradient force.

As in the Nakayama model with the constrained flow path, we assume nondivergent, irrotational flow around the vertical wall, defined by a stream function ψ by

$$\psi = -axz, \tag{7}$$

where ψ is zero along the x and z coordinates, and a is a positive or negative coefficient which depends only on time. The contour of a constant ψ, becomes a hyperbolic function. The wind vector of u and w is computed from ψ as

$$u = -\frac{\partial \psi}{\partial z} = ax, \quad w = \frac{\partial \psi}{\partial x} = -az. \tag{8}$$

Once the pressure gradient is determined from the temperature distribution, the coefficient a can be determined by taking the domain average of the pressure gradient force in (1) in the talus.

Figure 3 illustrates the vertical cross sections of the model configuration, and the examples of the stream functions for (a) August 7 (day 219), and (b) December 23 (day 357) at 0300 LST. The 2D model domain is given by $N\Delta x = 240$ m and $N\Delta z = 120$ m, with the grid size $N = 40$. The lower left and upper right triangles represent the talus and outer air, respectively. The negative and positive values of stream function designate downward and upward flows, respectively. In this study, temperatures of the cold wind hole, warm wind hole, and interior talus are represented by the points at the distance $(192, 21)$, $(42, 96)$, and $(90, 45)$, respectively as marked by circles in Fig. 3.

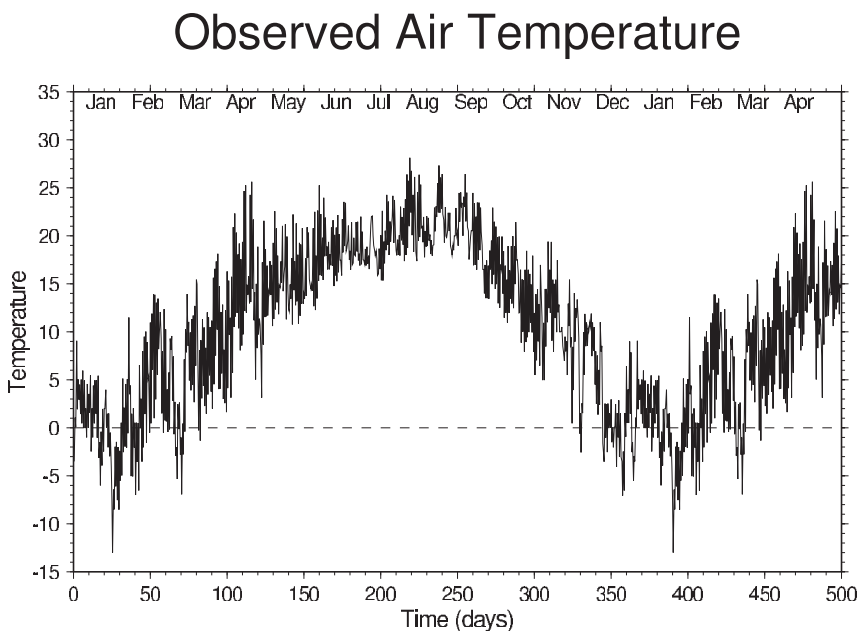

Fig. 4. Annual variation of observed outer air temperature (°C) at the Ice Valley in Milyang, Korea, for 500 days starting from January 1. Actual data are taken for one year from May 1, 2003 to April 30, 2004, which is used periodically for the input of the numerical model in this study (after Byun et al. 2004).

The stream function corresponds to the typical depth of the bed rock.

Base on the tracer experiments by Tanaka et al. (2004), we have adjusted the Rayleigh friction as $\nu = 15\ \mathrm{s}^{-1}$, to meet the observed wind speed. The air-rock mixing ratio $M = 0.001$, and the diffusion coefficient $K_a = 4.0 \times 10^{-3}\ \mathrm{m}^2/\mathrm{s}^2$, are determined accordingly, observing the computational results. Other parameters are the same as specified in Tanaka et al. (2000).

3. Ice Valley model experiment

3.1 Annual variation of temperatures

Annual variation of the observed outer air temperature at the Ice Valley in Milyang, Korea is plotted in Fig. 4 for 500 days starting from January 1. Actual data are taken for one year, from May 1, 2003 to April 30, 2004 (after Byun et al. 2004), which is used periodically for the input of the numerical model in this study. The outer air indicates a large diurnal variation, and passages of synoptic weather systems superimposed on the annual cycle. The annual mean temperature is 11.9°C, with the maximum 28.1°C and the minimum −13.0°C. The freezing temperature below 0°C is seen only for short periods in mid-winter.

Using the observed outer air temperature in Fig. 4, the model equation is integrated in time, starting from the initial condition of uniform temperature at 0000 LST, May 30, which is comparable to the annual mean. The time integration is conducted for more than 1000 days, with the time step of 60 sec. The outer air temperature over the talus is prescribed from the observation as in Fig. 4, while the interior temperature of the talus is predicted by the model.

Figure 5 shows the results of the annual variations of temperature at the cold wind hole (lower dashed line), warm wind hole (upper dashed line), and the interior of the talus (middle solid line) for 500 days, starting from January 1. Day 0 in the plot corresponds to day 580 after the initial condition. Also plotted is the observed outer air temperature (thin solid line) in Fig. 4. The overall features are quite similar to the in situ observations at Nakayama (Tanaka et al. 2000), and Ice Valley (Byun et al. 2004).

The temperature of the cold wind hole is lower than the freezing point in mid-winter. It

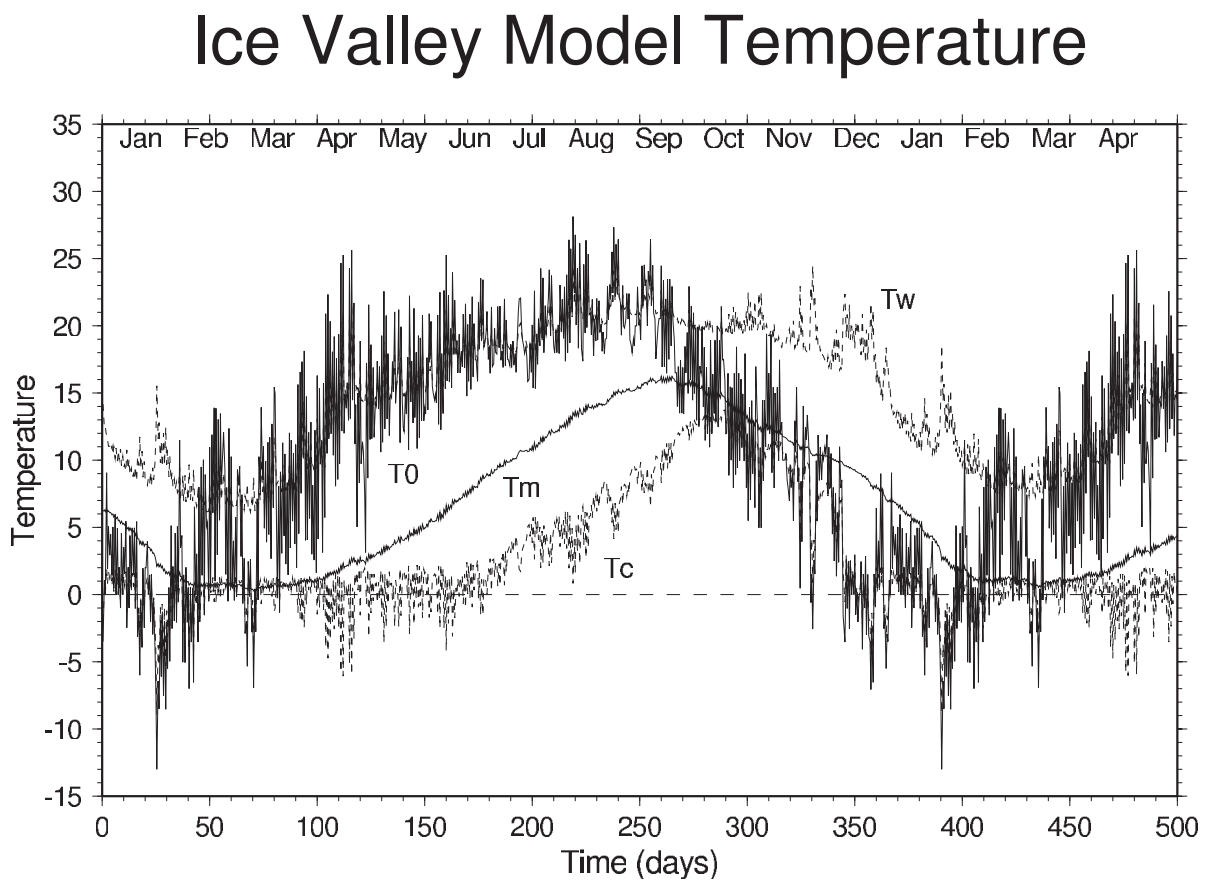

Fig. 5. Annual variations of model temperature (°C) at the cold wind hole (lower dashed line, T_C), warm wind hole (upper dashed line, T_W), and the interior of the talus (middle solid line, T_M) of the Ice Valley for 500 days starting from January 1. The observed outer air temperature (thin solid line, T_0) in Fig. 4 is also plotted.

keeps a minimum of 0°C till the day 180 (end of June). This is the period when ice persists in the cold wind holes. It then gradually warms, till the day 280 (beginning of October) reaching 13°C.

The warm wind hole shows the same temperature as the outer air during spring to summer, because it is the air intake. The summer is the period of cold wind-hole circulation, where warm outer air comes into the talus from the warm wind hole, and cooled air comes out from the cold wind hole. Temperature of the interior talus is seen between those of cold and warm wind holes. The warming speed is estimated as 2.0°C/month during summer.

The beginning of October is the time of the drastic turning point for the wind-hole circulation. Temperature of the cold wind hole intersects with the cooling outer air at about 12°C. Since the outer air is now colder than the interior talus, the downward wind circulation is replaced by upward wind circulation. The outer air comes into the talus from the cold wind hole at the foot of the talus and comes out from the warm wind hole at the top of the talus. We will refer to it as the warm wind-hole circulation.

It is important to note that the colder the outside air is, the stronger the warm wind-hole circulation is, blowing warm air from the warm wind hole, as seen for days 340 to 360. Since the warm wind hole circulation is the strongest during the night, the temperature of the cold wind hole during the night is almost the

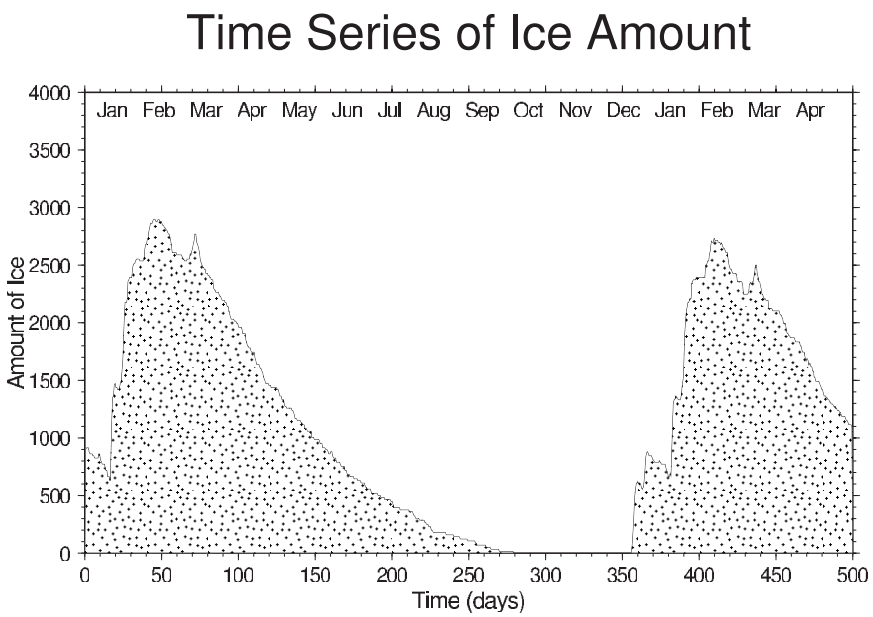

Fig. 6. Seasonal variation of the estimated ice amount (m^2) in the talus. The amount is represented by the number of pixels multiplied by the area of the grid size along the cross section.

same as the outer air temperature. During the warmer daytime, in contrast, the upward wind circulation is reduced, so the warmer air does not come into the talus, as seen for days 370 to 380. This property is consistent with the observations by Hwang et al. (2005) for the Ice Valley, and by Tanaka et al. (2000) for Nakayama Wind Hole. Namely, only the extreme cold in mid-winter can penetrate efficiently into the talus, as seen for January to February.

As a season progresses, the outer air gradually warms, and in March another turning point comes, to reverse the wind-hole circulation. The warm wind hole starts to suck the outer air. At the same time, the cold wind hole starts to blow freezing cold air. A very interesting response to the temporal warm weather is observed during days 100 to 120 (end of April) in Fig. 5. We can notice that the two lines for the outer air, and the cold wind hole, vary out of phase during this period. Namely, the cold wind hole freezes when the outside warms up to 25°C. In other words, the hotter the outside air is, the colder the wind hole is, as documented for the mystery of the Ice Valley. The amount of ice certainly increases near the cold wind hole in the model during this period. The numerical simulation provides us a great insight about the mechanism of the Ice Valley's ice.

Seasonal variation of the estimated ice amount in the talus is plotted in Fig. 6. The amount is represented by the number of pixels multiplied by the area of the grid size along the cross section. According to the result, the amount reaches its maximum in February and decreases monotonically to disappear in October. Although the amount decreased as a whole, it is confirmed that new ice forms at a small fraction near the cold wind hole on day 160, when the outer air warms up. New ice starts to form on day 356, when the first cold air outbreak occurs in December.

3.2 Annual variation of wind-hole circulation

Figure 7 shows the annual variation of wind speed (mm/s) along the stream line at the interior of the talus for 500 days, starting from January 1. The positive values represent the downward wind, and the negative values represent the upward wind. The annual variation of the wind speed is parallel to that of outer air temperature in Fig. 4. The downward wind of the cold wind-hole circulation begins at day 80 (mid March) and ends at day 270 (end of September). The maximum wind speed of 17 mm/s

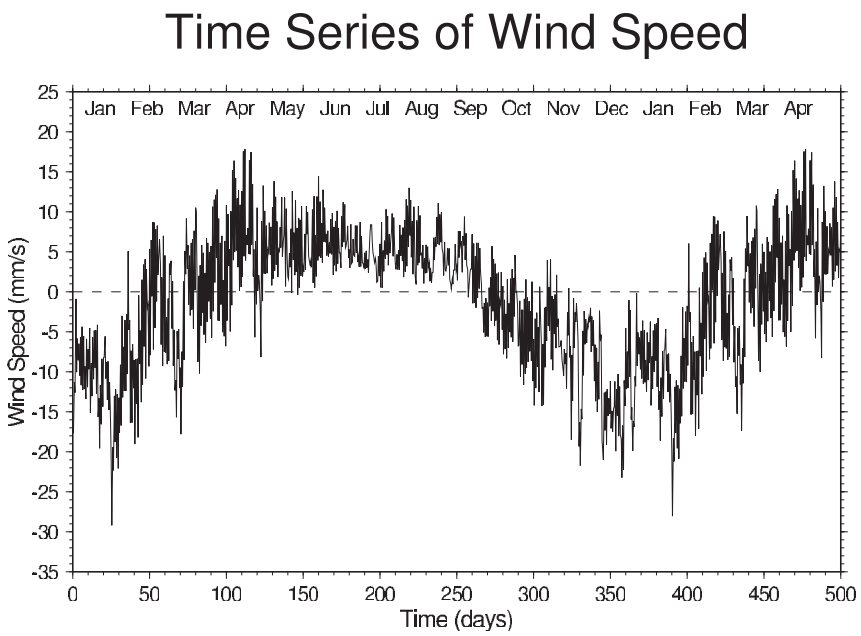

Fig. 7. Annual variation of wind speed (mm/s) at the interior of the talus for 500 days starting from January 1.

is seen at day 110 (mid April). Since the flow path is approximately 170 m, the mean residence time is estimated as 2.8 hours for this case. The downward wind blows gently, with about 5 mm/s during summer. The upward wind of the warm wind-hole circulation begins at day 270, and ends at day 80 with an exception for the temporal warming at days 50 to 60. The maximum wind speed of 30 mm/s is seen at day 25 when the outer air is the coldest. For this velocity, the residence time is estimated as 1.6 hours. Although the violent convective overturning is forbidden in the present model, in spite of the unstable stratification in winter, the mean upward wind in winter is clearly stronger than that of the mean downward wind in summer.

Using the annual variation of the wind speed, which represents the non-divergent mass flux along the constant stream function, we can evaluate the sensible heat flux, associated with the wind-hole circulations. Figure 8 illustrates the net sensible heat flux, evaluated as the sum of the sensible heat fluxes at the cold and warm wind holes. The positive value represents the accumulation of heat energy in the talus. According to the result, heat energy is accumulated in the talus during spring to summer, indicating the maximum of 600 W/m^2, and the typical value of 150 W/m^2. On the contrary, heat energy is released during winter indicating the maximum of 900 W/m^2, and the typical value of 300 W/m^2. Large amount of heat is released, i.e., winter cold is accumulated, by the temporal cold event for days 340 to 360, and for 385 to 395 in December and January. The value of 300 W/m^2 is twice larger than the ground heat flux of 150 W/m^2 observed at Nakayama by Tanaka et al. (2004).

The result quantitatively suggests that the convection theory represented by the seasonally varying wind-hole circulations, is sufficient to explain the mechanism of the Ice Valley's ice, which forms in spring and summer. The present study demonstrates that the violent convective overturning in mid winter is not necessary to accumulate the winter cold in the talus.

3.3 Vertical cross sections

Vertical cross sections of soil temperature in the model are illustrated in Fig. 9 for (a) April 16 (day 106), (b) August 7 (day 219), (c) October 15 (day 288), and (d) December 23 (day 357) at 0300 LST.

On April 16 (day 106), the freezing area is

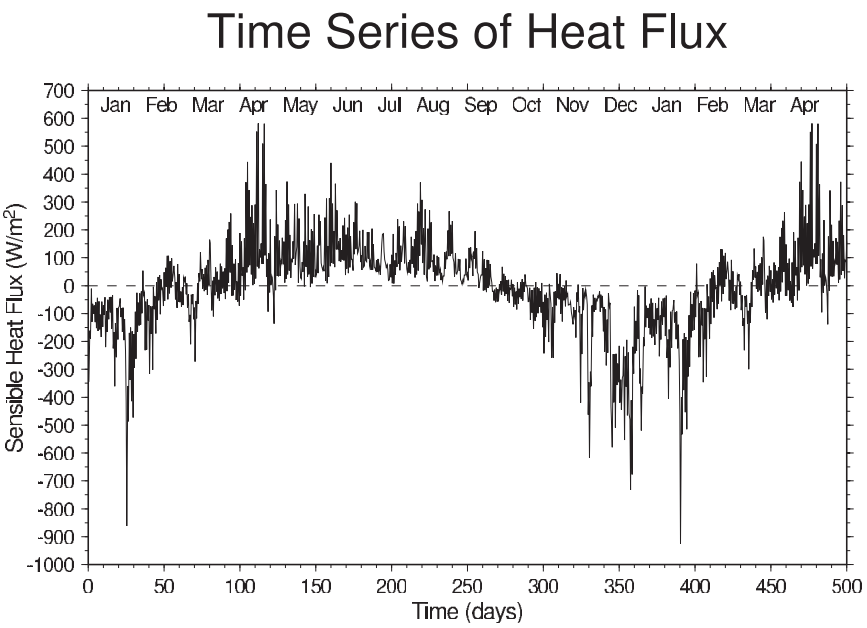

Fig. 8. Annual variation of the net sensible heat flux (W/m^2) for the talus evaluated as the sum of the sensible heat fluxes at the cold and warm wind holes for 500 days starting from January 1.

seen at the lower end of the talus, as marked by square symbols. Uniform 0°C area implies existence of ice. Outer air temperature is about 14°C. It is just after the onset of the downward flow. The left half of the talus is warmer than the right half of the talus, and the warming area gradually expands downward from the upper part of the talus.

On August 7 (day 219), the outer air is about 22°C. The downward flow is in full strength. The upper talus is heated to more than 20°C, and the warming area keeps expanding downward. Still, a cold area with ice remains at the lower end of the talus.

On October 15 (day 288), the outer air cools down to 15°C. The cold area seen at the lower end of the talus has disappeared. The interior talus has been warmed during summer, which is now cooled from the surface of the upper slope of the talus. The warm belt is formed about 10 m depth from the surface. An isolated cold area, of 4°C, is seen at the bottom of the model domain, near 160 m distance. As the upward flow intensifies, the talus is cooled from the lower surface.

On December 23 (day 357), the outer air temperature cools down to about −3°C. The cold outer air is sucked from the lower surface of the talus by the upward wind. The freezing area appears at the lower surface, and expands into the talus, pushing the warm air at the left side of the talus. The cold air undergoes strong warming as soon as the air comes into the talus, due to the large temperature gradient. The relative humidity would drop rapidly as the cold air moves into the talus. Snow or ice near the surface would soon disappear by the sublimation under such a dry condition as mentioned by Byun et al. (2006). If there is no water or ice by the sublimation, the temperature goes down below the freezing point, to accumulate the winter cold into the dry rocks.

Figure 10 illustrates the vertical cross section for January 25 (day 391), when the outer air is the coldest, −13°C. The freezing area expands into the lower talus and the temperature distribution shifts to that of April 16 (day 106) described above. It is demonstrated that the winter cold is accumulated effectively in the talus during the event of the cold air outbreak in a short time. The result described in this subsection is basically similar to that of the Nakayama model, discussed by Tanaka et al. (2000), although the model is driven by the observed outer air temperature at the Ice Valley in Korea.

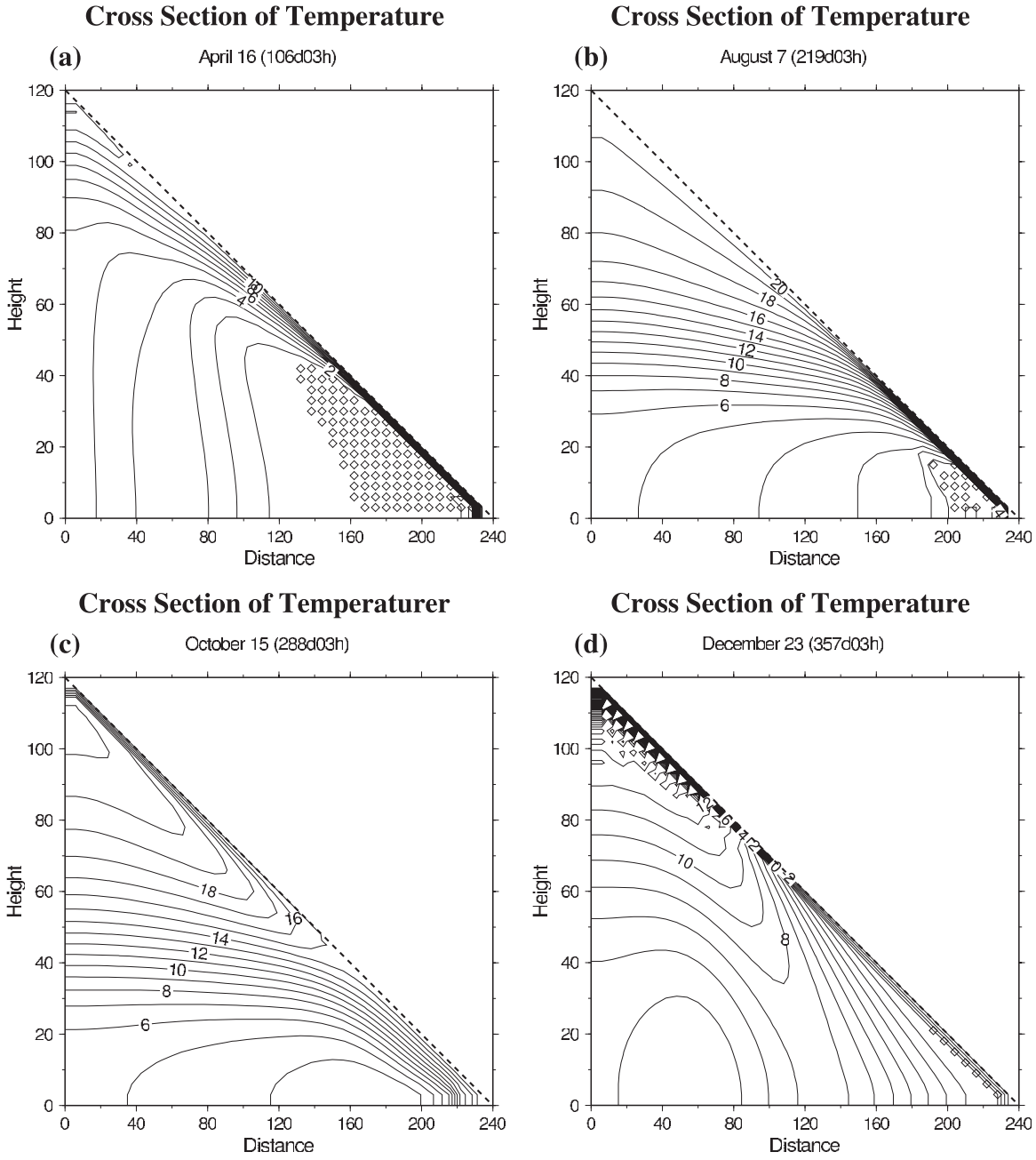

Fig. 9. Vertical cross sections of soil temperature (°C) in the model for (a) April 16 (day 106), (b) August 7 (day 219), (c) October 15 (day 288), and (d) December 23 (day 357) at 0300 LST. Square symbols represent the location of ice in the model.

4. Concluding summary

The Ice Valley in Korea is a famous summer resort, where natural ice forms in spring and summer, and the ice disappears in fall and winter. It is interesting to note that the hotter the outside air is, the larger the ice grows in spring, as documented by Kim (1968). The mysterious behavior of the summertime ice has been explained by a series of numerical experiments

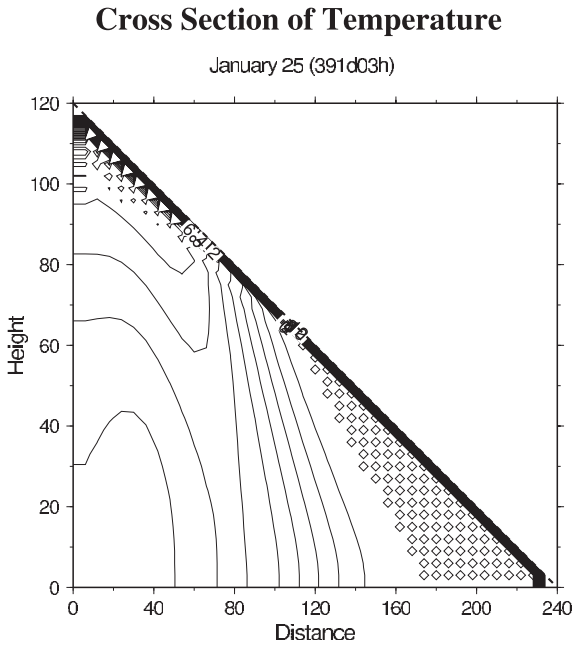

Fig. 10. Vertical cross sections of soil temperature (°C) in the model for January 25 (day 391) at 0300 LST when the outer air is the coldest in a year with −13°C.

by Tanaka et al. (2000) in terms of the convection theory, with the seasonal reversal of wind-hole circulations.

However, the subsequent tracer experiments of the wind-hole circulation by Tanaka et al. (2004), showed that the wind speed in the talus is about 26 mm/s, which is on order of magnitude larger than that inferred by the model experiments. Moreover, the comprehensive in situ observations at the Ice Valley by Byun et al. (2004), found that there are persistent warm wind holes during winter, which contradicts with our former Ice Valley model. In the former Ice Valley model, the active overturning of the unstably stratified air in the talus resulted in too much freezing of the entire talus, destroying the persistent warm wind hole. The characteristics of the observed warm wind holes at the Ice Valley are rather similar to the result of the Nakayama model, where the wind-hole circulation is constrained along a fixed stream line. For these reasons the Ice Valley model is updated in this study, based on the new findings by the in situ observations.

In this study, numerical simulations of the wind-hole circulation at Ice Valley in Korea are conducted using a simple 2D model, which is driven by the annual march of the observed air temperature. The result of the simulation is compared with the in situ observations at Ice Valley in Korea (Byun et al. 2004), and at Nakayama in Japan (Tanaka et al. 2000).

According to the results of the numerical simulations, the summertime wind-hole circulation intensifies the downward flow when the outside air is getting hot. The downward flow transfers the cold accumulated in the talus to the outlet of the cold wind hole. As a result, the intensified cold advection grows the ice when the outside air is getting hot.

In contrast with our former simulations, we demonstrated that the wind hole circulation reaches 17 mm/s in April, and the residence time of the air in the talus is about 2.8 hours for this case. It is found that the seasonal reversal of the wind hole circulations acts as a thermal filter, which accumulates only the winter cold in the talus, and the accumulated cold grows the springtime ice of the Ice Valley. We may say that the ice of the Ice Valley is no longer a mystery. This study has demonstrated that the violent convective overturning in midwinter is not necessary to accumulate the winter cold in the talus.

The results of the present study are, however, sensitive to the model parameters, and still contradict with observations in the persistence and steadiness of the warm wind hole in winter. The assumption of the hyperbolic stream function must be modified by geological investigations. The actual Ice Valley has a 3D flow pattern with effective convergence of downward flow near the outlet of the cold wind hole. The 3D features of the complete Ice Valley model may be the future subject of the numerical model simulation. It is desired also to perform observations for the interior of the talus by digging a hole in order to support the model speculations. Finally, the role of surface radiation, moisture, condensation, and evaporation, which have been ignored in this study, must be considered in a future study.

Acknowledgments

The authors appreciate the staff and students at the Pukyon National University for the support of the observations at the Ice

Valley. The study is supported by the International Arctic Research Center (IARC/UAF) and by Asahi Breweries Foundation. The first author acknowledges Ms. Honda for her technical assistance. The third author was supported by the Korea Meteorological Administration Research and Development Program under Grant CATER 2006–2306. The authors are also grateful to Miryang city for providing conveniences to observe.

References

Bae, S.K. and Kayane, I., 1986: Hydrological study of Ice Valley, Korea. *Ann. Rep., Inst. Geosci., Univ. Tsukuba*, **12**, 15–20.

Byun, H.-R., K.-S. Choi, K.-H. Kim, and H.L. Tanaka, 2004: The characteristics and thermal mechanism of the warm wind hole found at the Ice Valley in Mt. Jaeyak. *J. Korean Meteor. Soc.*, **40**, 453–465.

——— and 22 persons, 2006: *Study on the mechanism of the summertime icing on the Ice-Valley*. Miryang city Kyeong-Nam, Korea, 402 pp.

Hwang, S.-J. and S.-E. Moon, 1981: On the summertime ice formation at Ice Valley in Milyang, Korea. Abstracts in Spring Conference, *Geographical Soc. Japan*, **19**, 218–219.

———, K.-S. Seo, and S.-H. Lee, 2005: Study on ice formation mechanism at the Ice Valley in Milyang, Korea. *J. Korean Meteor. Soc.*, **41**, 29–40.

Kim, S.-S., 1968: On the ice-formation at the "Ice-Valley", Milyang Koon, Korea in summer season. *J. Korean Meteor. Soc.*, **4**, 13–18.

Moon, S.-E. and S.-J. Hwang, 1977: On the reason of the ice-formation at the Ice-Valley, Milyang Kun, Korea in the summer season. *Pusan National University, Paper Collections*, **4**, 47–57 (in Korea with English abstract).

Song, T.-H. 1994: Numerical simulation of seasonal convection in an inclined talus. *Proc. 10th Intl. Heat Transfer Conf.* Brighton, UK. Vol. 2, 455–460.

Tanaka, H.L. 1995: Mysterious ice valley in Korea where ice grows during the hottest season. *Tenki*, **42**, 647–649 (in Japanese).

——— 1997: A numerical simulation of summertime ice formation in the Ice Valley in Milyang, Korea. *Geogr. Rev. Japan*, **70A**-1, 1–14 (in Japanese with English abstract).

———, Moon, S.-E., and Hwang, S.-J. 1998: Mysterious ice valley in Korea where ice grows during the hottest season. *Tenki*, **45**, No. 11 Color Pages, 3–4 (in Japanese).

———, ———, and ——— 1999: An observational study of summertime ice formation at the Ice Valley in Milyang, Korea. *Sci. Rep., Inst. Geosci., Univ. Tsukuba*, **20**, 33–51.

———, D. Nohara, and M. Yokoi, 2000: Numerical simulations of wind hole circulations and summertime ice formation at Ice Valley in Korea and Nakayama in Fukushima, Japan. *J. Meteor. Soc. Japan*, **78**, 611–630.

———, N. Mura, and D. Nohara, 2004: Mechanism of cold air vent at the Nakayama windhole in Shimogo, Fukushima. *Geogr. Rev. Japan*, **77**, 1, 1–18 (in Japanese with English abstract).